QUANTIFYING UNCERTAINTIES IN THERMOELASTIC PREDICTIONS

Simon Appel[(1)], Alberto Peman[(2)], Jaap Wijker [(3)], Alexander van Oostrum[(2)]

[(1)] ATG Europe for ESA, Keplerlaan 1, 2201AZ, Noordwijk (ZH), The Netherlands,
Email: Simon.Appel@esa.int
[(2)] ATG Europe, Huygensstraat 34, 2201 DK Noordwijk (ZH), The Netherlands
Email: Alberto.Peman@atg-europe.com / Alexander.vanOostrum@atg-europe.com
[(3)] Ronde Zonnedauw 17, 1991 HT Velserbroek, The Netherlands,
Email: j.j.wijker@hetnet.nl

KEYWORDS

Thermoelastic, uncertainties, margin-policy

ABSTRACT

A thermoelastic analysis is a multi-step process with multiple disciplines involved where each discipline uses its own mathematical model. Each of the models involved is a source of uncertainties and errors. In addition, there are also the errors coming from the data transfer and transformation between the different analysis steps.

To account for these uncertainties, factors of safety, can be used. Although this approach is pragmatic, it suffers from a lack of reliability basis and the values are often ambiguous.

Stochastic approaches are powerful for quantifying ranges in the responses due to variations of parameters. The Monte Carlo Simulation (MCS) method is a well-known method for this purpose, but it is computationally expensive. A promising alternative method is the Rosenblueth Two-point estimate method, that requires far less computational effort.

This paper explains the application of the Rosenblueth method for estimation of the uncertainty of thermoelastic prediction. This explanation is supported with examples.

1 SOURCES OF UNCERTAINTIES IN THERMOELASTIC ANALYSIS AND USE OF FACTORS OF SAFETY

The thermoelastic analysis process is a chain of analysis steps, in which each step introduces uncertainties. A common way to deal with above uncertainties is to introduce factors similar to the ECSS "Structural factors of safety for spaceflight hardware" [6].

In the thermal model typical parameters with uncertainty are thermo-optical properties and contact conductance values. Also, the thermal environment may have some variations from the assumed nominal environment. In addition, the reflection of solar and infra-red radiation from surrounding objects on the spacecraft may cause uncertainties in the heat radiation received by the structure under consideration. The ECSS “Thermal analysis handbook” [8] provides an overview of potential uncertainty sources.

The uncertainties in the thermal model can be covered with the thermal model factor K_{mt}. This factor will then act as a scaling factor for the thermoelastic (TE) responses, like stresses and displacements. Similar to the thermal model factor, a thermal environment factor, K_{et}, may be introduced that also scales the thermoelastic responses.

Temperature mapping from the thermal model to the structural model is the second step in the analysis chain. A mismatch in the level of detail between the thermal and structural model can be a source of errors. This source can be removed to a large extent by putting the right amount effort on aligning the models. Also, a mismatch between mesh boundaries, can cause partial overlap of elements by thermal nodes. With some effort this problem can be minimised, but not always removed. Finally, the selected temperature mapping method can be a source of uncertainties by itself. A factor of safety, K_{map}, for the temperature mapping process can be introduced to cover the uncertainties for this analysis step.

The structural model, like the thermal model, uses a large amount of material properties and geometrical dimensions which all have their own variation around their nominal value. The factor that could cover the uncertainties in the structural thermoelastic model can be K_{ms}.

In principle, a factor of safety for the performance evaluation of the instrument could also be introduced. This aspect is considered outside the scope of this paper.

The cumulative effect of these factors could be presented as a single thermoelastic factor of safety K_{te}

$$K_{te} = K_{mt}K_{et}K_{map}K_{ms} \qquad (1)$$

Like with the factors $K_m$and K_p, as proposed by the ECSS [6], there is no reliability basis for quantifying the previously introduced factors of safety. The

chosen values then rely on experience, which is not always available. The factors may also be the result of a compromise between customer and contractor. As a consequence, the values have a high level of ambiguity.

Despite that factors of safety are meant to introduce a level of conservatism in the results, they actually generate a false sense of safety.

Although the use factors of safety is a pragmatic approach, it also has some limitations and brings additional uncertainties. For those reasons in the next section an alternative to the approach with factors of safety is discussed to deal with uncertainties. Different from the factors of safety approach, an efficient stochastic method is described, that allows to estimate the uncertainty in the results based on the mean and standard deviation of physical parameters in the models.

2 UNCERTAIN DESIGN VARIABLES, PROBABILISTIC APPROACH

In section 1 the traditional way to cover uncertainties in the environment and modelling parameters by factors of safety was discussed. In this section uncertainties in applied loads and design variables are considered as stochastic or random parameters.

Stochastic design variables may have different distribution types, such as normal and log-normal. [2,3]. In cases where the distribution is not known, a uniform distribution $U(a,b)$ with a specified interval (a,b) could be used.

The outcomes of the probabilistic analysis are statistical values, e.g. the mean μ, the standard deviation σ.

In this paper two probabilistic analysis methods are discussed:

- Monte Carlo Simulation (MCS) [2,3]
- Rosenblueth's $2k+1$ Point Estimate Method (PEM) [1,2,5]

The emphasis of this paper is on the latter method, that is believed to be an interesting alternative for the MCS method. The $2k+1$ PEM method can be considered as computationally light method that has the potential to make stochastic assessments possible within projects with high schedule constraints.

2.1 Monte Carlo Simulation (MCS)

To assess the stochastic properties of the response variables with the MCS method a (very) large number of simulations runs have to be done, sampling the design variables and loads stochastically. The following steps must be done:

- Definition of reliable mathematical models
- Selection of stochastic design variables
- Generation of memoryless[1] random numbers in conjunction with the selected distribution
- Evaluation of stochastic response variables
- Statistical analysis

The accuracy of the MCS analysis will improve with the number analysis loops. After all evaluations of the response variables, the mean μ, the standard deviation σ, the distribution, minimum and maximum values can be estimated.

MCS is easy to implement but is, in general, computationally expensive.

2.2 Rosenblueth's $2k+1$ Point Estimate Method (PEM)

With the use of the Rosenblueth point estimates for first and second order probability moments [1,2,5], estimates of the mean and the variance of the stochastic response variable in combination with a mathematical model can be computed. The interesting feature of this method is that, when the number of stochastic design variables is k, the number of analysis runs, for computation of the estimates is limited to $2k+1$.

The response is considered to be a function of all the design variables:

$$Y = Y(X_1, X_2, \dots, X_k), \qquad (2)$$

with $X_n (n \in [1,k])$ being stochastic design variables. Each design variable X_n has a mean value μ_n and standard deviation σ_n. To produce a response value Y a single analysis run is required.

The $2k+1$ response values, thus analysis runs, are the following:

- $Y_0 = Y(\mu_1, \mu_2, \dots, \mu_k)$: The nominal or reference value of the response computed by using the mean values μ for all k stochastic design variables.
- $Y_{nm} = Y(\mu_1, \mu_2, \dots, \mu_n - \sigma_n, \dots \mu_k)$: The response resulting from k analyses in which all values of the response variables are kept at their mean value μ, except the n^{th} stochastic design variable that is set to the value $\mu_n - \sigma_n$ (m means minus)
- $Y_{np} = Y(\mu_1, \mu_2, \dots, \mu_n + \sigma_n, \dots \mu_k)$: The response resulting from k analyses in which all values of the response variables are kept at their mean value μ, except the n^{th} stochastic design variable that is set to the value $\mu_n + \sigma_n$ (p means plus)

The mean Y_n of two-point estimates Y_{nm} and Y_{np} is given by,

[1] Note that for the generation of random numbers it is not verified whether a certain combination of design variable values has been used before. That is why the generation of random numbers is called memoryless.

$$Y_n = \frac{Y_{nm} + Y_{np}}{2}, n = 1,2, \cdots k \quad (3)$$

and the coefficient of variance V_n can be obtained by,

$$V_n = \frac{Y_{np} - Y_{nm}}{Y_{np} + Y_{nm}}, n = 1,2, \ldots k \quad (4)$$

Assuming all stochastic design variables are uncorrelated and non-skew the following estimates of the mean $\bar{Y} = \mu_y$ and the coefficient of variance $V_y = \sigma_y/\mu_y$ can be calculated with

$$\frac{\bar{Y}}{Y_o} = \prod_{n=1}^{k} \frac{Y_n}{Y_o} \quad (5)$$

and

$$1 + V_y^2 = \prod_{n=1}^{k} (1 + V_n^2) \quad (6)$$

The values of V_n of equation (4) can be used as a sensitivity value of the design variables on the response variable(s). When all the coefficients of variation are normalised relative to the coefficient of variation for the response value, individual sensitivity index values can be obtained,

$$S_n = \frac{V_n}{V_Y}, \quad (7)$$

The sensitivity index values can provide useful information in identifying the parameters driving the uncertainty.

It should be noted, that the PEM is based on a truncated Taylor's series. For this reason, Rosenblueth stresses several times in his paper [1] that the dispersion of the stochastic design variables should not be "too large". Rosenblueth is not specific about the quantification of "too large". This constraint may indicate that the accuracy has a sensitivity for the magnitude of the dispersion of the stochastic design variable.

3 DEMONSTSTRATION CASES

In the following sections two demonstration cases are presented with the objective to show the practical use of the $2k + 1$ PEM method. The first example is a more realistic example that shows well the procedure to a design problem. The second example shows what can be done when limitations of the $2k + 1$ PEM method are hit.

3.1 Demo case 1: Simplified optical bench model

The purpose of this example was to investigate the effects that uncertainties in several parameters and modelling methods could introduce in an optical instrument's performance under TE loads.

3.1.1. Scope and limitations

In this investigation, various TE analyses were carried out. These TE analyses had to describe the performance of the optical bench in a thermal vacuum facility and provide deeper understanding on the effects that the uncertainty in several modelling parameters and modelling methods had on the results. Due to the random behaviour of uncertainties, the parameters under study were treated as stochastic variables. The TE analyses, therefore, became also statistical analyses. To perform these statistical analyses, both the Monte Carlo Simulation method and the $2k + 1$ PEM method, described previously, were used, and are compared at the end of it.

It is important to acknowledge that this example had several limitations. First, the thermal and structural models were simplified, inherited models from past studies [10]. Therefore, it is important to notice that they did not represent a real optical instrument, but they have features that can be found in realistic models. As they are theoretical models, another limitation is that there was no test data to compare the results with. This limits the conclusions that can be based on data trends. The last limitation is that only steady state cases were analysed and no transient cases.

3.1.2. Model description

The models used were based on features of common optical system payloads. As they were inherited from a previous study, in order to improve the models' suitability for the current study, some modifications were introduced.

The models can be subdivided into the parts shown in Figure 1. The main optical path in the instrument includes the front opening and its baffle, both mirrors and the focal plane assembly (FPA).

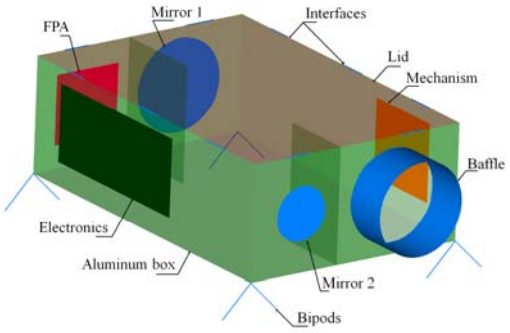

Figure 1: Optical payload model overview.

To avoid thermal gradients within the instrument everything except for the bipods was made of Al 6061-T6. The bipods were made of Ti-6Al-4V in order to thermally decouple the instrument from the spacecraft (SC) deck.

As shown in Figure 2, the outside surface of the GMM was covered in MLI, except for the radiators. To simplify the model, the volume of the different dissipating units has not been modelled. Therefore, in this case, the inside of each shell acted as the thermal node (TN) for the aluminium structure or mirrors and the external surface of the shell acted

as the TN for the MLI or radiators.

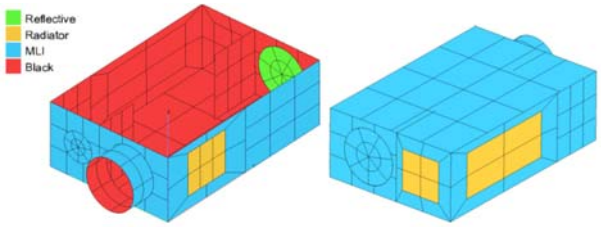

Figure 2: GMM thermal model components showing the optical properties of the optical payloads.

All the radiative conductors were automatically computed using ESATAN except for the conductors between the structure and the last MLI layer. These manually computed conductors were modelled using a tuned parameter: the effective emissivity (ε^*). This parameter measures the insulating efficiency of the MLI.

The linear conductors between TNs were generated using the automatic GL generation module from the SINAS software [10]. The use of this method introduces repeatability and reproducibility into the conductors as it removes the human experience factor from the level of accuracy of the conductors.

Figure 3 shows a 3D view of the FE model used in the structural part of the TE analysis. The rotation of both mirrors was chosen as a representative performance parameter. In this case, they were computed using an RBE3 element.

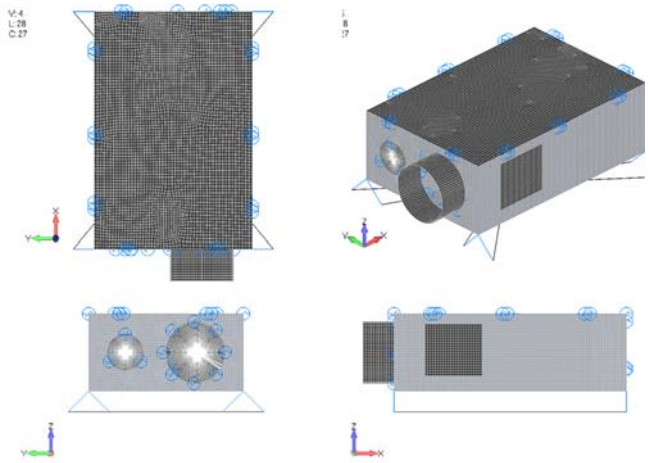

Figure 3: FE model 3 view.

3.1.3.Uncertain parameters and methods

For this study, one property from both the thermal and structural models have been treated as design variables.

From the thermal model, ε^* was chosen for this study due to the high degree of uncertainty that it commonly has in thermal analyses. From the structural model, the aluminium's CTE was chosen as the design parameter due to the CTE's importance in TE analyses.

As the models in this example are only theoretical, there is no data to determine the probabilistic distribution of these variables. Due to this issue, several assumptions were made. First, both random variables were modelled using a normal distribution. Due to the chosen distribution, to keep the random samples realistic the tails of these had to be cut-off at 3σ.

The mean value (μ) of ε^* was then modelled using a typical value. To estimate the standard deviation the value suggested by the ECSS thermal handbook was taken. The ECSS guidelines [8] recommend applying an uncertainty of ±50% for the MLI's effective emissivity before testing. Therefore, 0.5μ was taken as 3σ.

The CTE value for aluminium from the MIL-HDBK-5J handbook [11] was used as the mean value for the CTE's distribution. Yet the handbook does not provide a standard deviation value for its measurement; therefore, an extra assumption was made. In this case a large value of ±15% for the uncertainty of the aluminium's CTE value was chosen. As a result, 0.15μ was taken as 3σ. It is acknowledged that this value is extremely high for a material such as aluminium, but it is not rare in other materials.

Table 1 summarizes the properties of these two distributions.

Table 1 Statistical properties of the stochastic variables.

Parameter	Units	μ	3σ
ε^*	-	4.0E-2	2.0E-2
CTE	m/m/degC	2.360E-5	0.354E-5

To consider uncertainty in TE methods, all the studies were performed applying two common temperature mapping methods: centre point temperature (CPT) conductive interpolation method, and the prescribed average temperature method (PAT) (SINAS) method. A detailed description of these methods can be found in [9]. This was done to assess the influence of each method on the results of the analyses. As this is not the main focus of the current paper, they are not described further.

3.1.4.Analysis methods

Three different Monte Carlo simulations were carried out in this project:

- Analysis with a random CTE
- Analysis with a random ε^*
- Analysis with a random CTE and ε^*

This section only details the method that was followed for the last analysis as it is a combination of the previous two.

First, the random parameters were sampled. When doing so, it was considered that a single batch of aluminium was used to produce the structure. This

meant that only 1 CTE sample had to be taken per run. At the same time, three random samples of the ε^* were taken for three different locations. This was done to account for the dependence of ε^* on the packaging of the MLI [12]. Therefore, in total, 4 random samples were computed for the design variables per Monte Carlo run.

After performing the sampling, for each run, a thermal analysis was computed to consider the changes in ε^*. The new temperature field was then mapped onto the structural model using the 2 different mapping methods. Following the temperature mapping, a structural analysis was computed on the FE structure and the results for the performance parameters measured.

This process was carried out in sets of 50 cases. After each set, the mean and standard deviation of the performance parameters were computed. When the mean and standard deviations converged within 1% and 5%, respectively, the process was stopped.

After the Monte Carlo simulation, the $2k+1$ PEM method analysis was performed following the instructions given in section 2.2. In this case, as there were 4 different design parameters (3 different ε^* and 1 CTE) a total of 9 cases were run.

3.1.5.Results

Due to the non-linearity of the radiative effects in the thermal analyses it could not be directly extrapolated that given the normal distribution of the random samples the results would also be normally distributed. Therefore, a Jarque-Bera (JB) normality test was computed on the distribution of the performance parameters [13].

As the Monte Carlo simulations showed little skewness and that they passed the normality test, with a 95% confidence level, the results from the $2k+1$ PEM method were also assumed to belong to a normal population.

This assumption allowed us to represent both distributions together. The results of both simulations are displayed in Figure 4. This figure shows that the $2k+1$ PEM method can capture the behaviour of the performance parameters just as the Monte Carlo Simulations do. Table 2 and Table 3 summarise the difference between the estimators of both methods.

These relative differences use the results from the Monte Carlo method as the baseline case,

$$\Delta \mathrm{Y} = \frac{\overline{\mathrm{Y}}_{MonteCarlo} - \overline{\mathrm{Y}}_{Rosenblueth}}{\overline{\mathrm{Y}}_{MonteCarlo}} \tag{8}$$

$$\Delta \mathrm{S_Y} = \frac{S_{Y\,MonteCarlo} - \sigma_{Y\,Rosenblueth}}{S_{Y\,MonteCarlo}} \tag{9}$$

The results show how the $2k+1$ PEM method estimated the mean of the outputs' distribution with great precision. The percentage difference between the mean values was always within the relative width (wr) of the confidence interval for the baseline's mean.

It is also interesting to note that, the estimate for the standard deviation of the population does not show the same level of precision.

Still, it is important to mention that all the results computed with the $2k+1$ PEM method fall within the confidence intervals of the Monte Carlo simulation results.

Table 2 Percentage difference in the distribution estimators between the results obtained with the Monte Carlo simulation method and the Rosenblueth 2k+1 estimates method. (Rotation around the Y axis)

	Mirror 1		Mirror 2	
Estimator	**SINAS (PAT)**	**Conductive (CPT)**	**SINAS (PAT)**	**Conductive (CPT)**
$\Delta \mathrm{Y}$ [%]	0.151	0.146	0.076	0.072
$\Delta \mathrm{S_Y}$ [%]	6.178	5.691	5.007	4.288

Table 3 Percentage difference in the distribution estimators between the results obtained with the Monte Carlo simulation method and the Rosenblueth 2k+1 estimates method. (Rotation around the Z axis)

	Mirror 1		Mirror 2	
Estimator	**SINAS (PAT)**	**Conductive (CPT)**	**SINAS (PAT)**	**Conductive (CPT)**
$\Delta \mathrm{Y}$ [%]	0.096	0.096	0.003	0.007
$\Delta \mathrm{S_Y}$ [%]	4.824	5.110	2.055	1.309

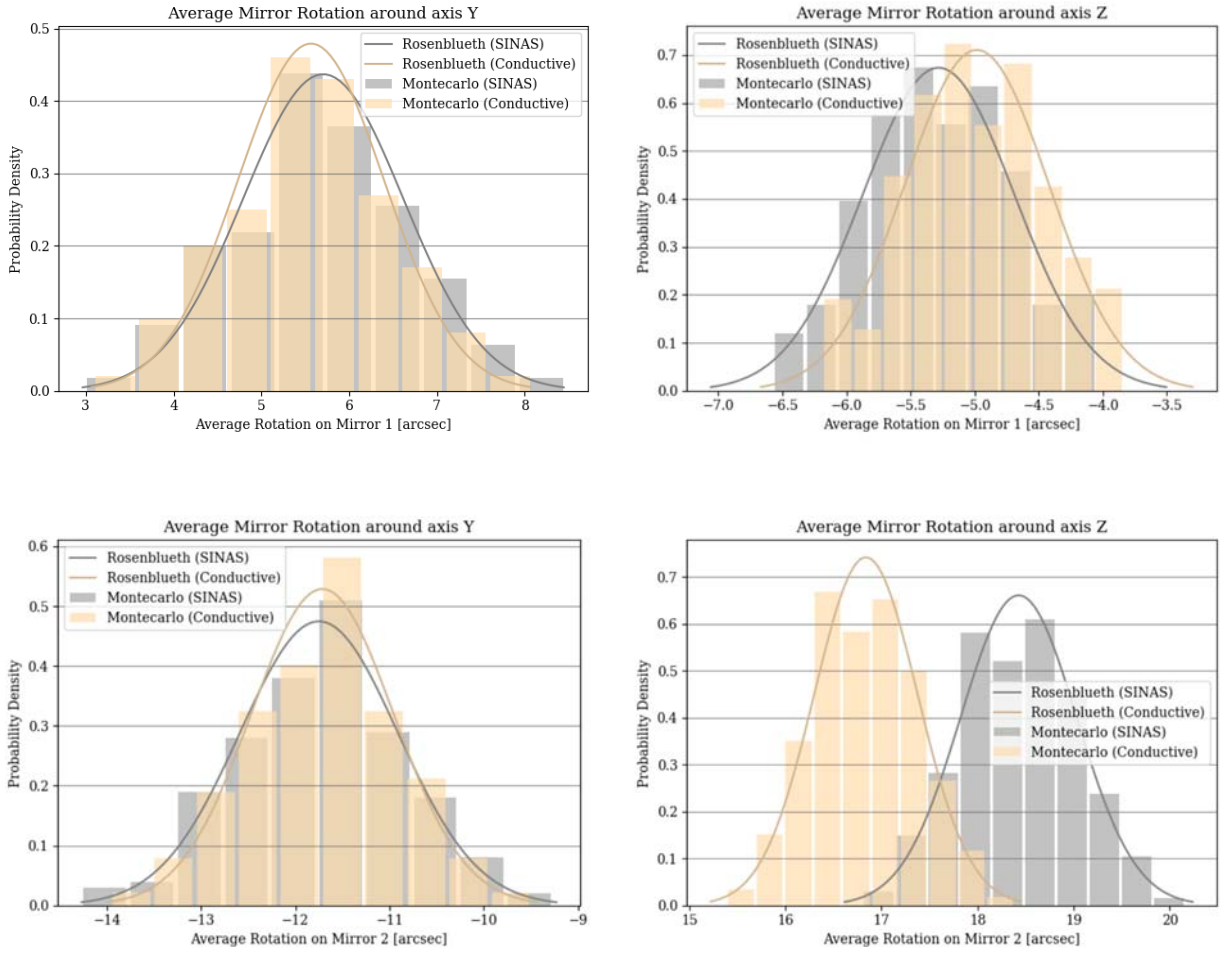

Figure 4: Overlap of the CTE, effective emissivity Monte Carlo simulation and the $2k+1$ PEM method (Rosenblueth) estimates results.

3.1.6.Conclusions

Several conclusions can be extracted from the results.

Firstly, the $2k+1$ PEM method shows a great level of precision when predicting the mean value of the population for this case. The results from the $2k+1$ PEM method, all fall within less than 0.2% of the mean computed through the Monte Carlo Simulation method. It is important to mention that this was achieved using a fraction of the computational time. Furthermore, even though the variability of the population shows a lower precision it still falls within the 95% confidence intervals from the Monte Carlo Simulation results. This means, that the $2k+1$ PEM method could have been used with great precision to assess the effects of random uncertainties in this case.

It is also important to note, that as seen in the results, the mapping methods can heavily influence the estimated means of our distributions. As this was not the purpose of this paper, this is not considered further.

3.2 Demo case 2: PANELSAT

3.2.1 Model description

PANELSAT is a fictitious satellite which consists of only a rectangular sandwich panel. The example with PANELSAT aims to show the application of the Point Estimates Method (PEM) of Rosenblueth of section 2.2 in combination with the Monte Carlo Simulation method (MCS) of which the results are used as reference. It should be understood that a single panel orbiting around a planet has no resemblance with any of the current spacecraft.

The sandwich panel is 1 × 2 m and has a thickness of 5 cm. The sandwich has aluminium face sheets of 1 mm thickness and aluminium honeycomb core material.

The MSC.Nastran finite element model is presented in Figure 5 The face sheets and edges of the panel are modelled with linear shell elements (CQUAD4). The core is modelled with linear solid elements (CHEXA). The shell elements are coinciding with the free faces of the solid elements representing the honeycomb core. A perfect joint between face sheets and core is assumed and the adhesive between core and face sheets is omitted.

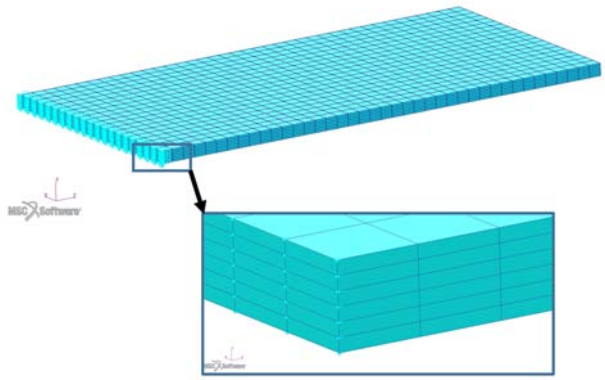

Figure 5 PANELSAT FE model with boundary conditions indicated. Lower part: Detail showing the high through thickness mesh resolution.

The panel is orbiting around Earth in a polar orbit with the +Y side of the panel pointing in the nadir direction.

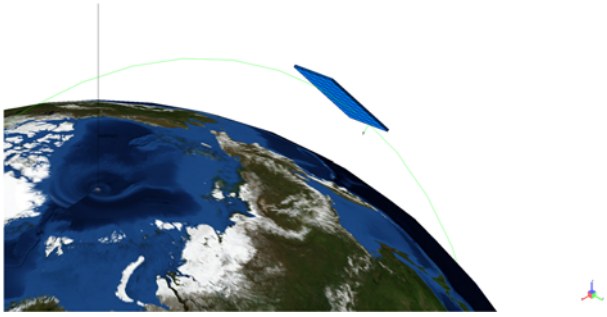

Figure 6 PANELSAT orbiting around Earth with +Y axis nadir pointing.

An infrared emissivity of $\varepsilon = 0.5$ (-) is used for the +Y side and $\varepsilon = 0.8$ (-) is used for the remaining surfaces. The solar absorptivity for the +Y side is $\alpha = 0.5$ (-) and $\alpha = 0.2$ (-) for the remaining surfaces. The edges have the same thermo-optical properties as the zenith surface.

In the simulation process for this example, the conductors between thermal nodes are computed with the method based on the PAT relations as explained in [7].

3.2.2 Nominal results

It is assumed that the models that are used for this example have gone successfully through the convergence verification.

As a result of the changing orientation to the sun in combination with entry and exit of eclipse, the temperature field is constantly changing with time with corresponding changes in deformation. The translation of the mid-point of the +Z edge of the panel is (for the sake of the example) considered important for the performance of PANELSAT. This translation is relative to the clamped boundary condition at the -Z side of the panel.

In Figure 7 the variation of the tip displacement over two orbits is visualised together with the temperature evolution at the middle of the panel at the two opposite face sheets at corresponding moments in time. The figure shows strong variations in displacement as function of time. The displacements vary between -0.195 mm and -1.25 mm. The steep slopes in the displacement curves coincide with moments of increased temperature difference between top and bottom skin that occur during entry and exit of eclipse. In Figure 7 the coinciding of the moments of strong variation of the tip displacements and increased temperature difference between top (nadir) and bottom (zenith) face sheet is indicated with dotted lines.

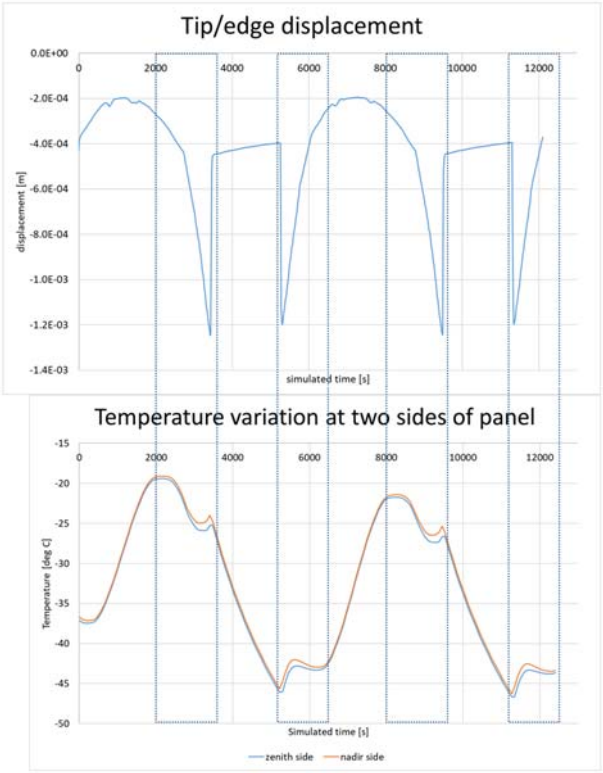

Figure 7 As a function of time the PANELSAT tip edge displacement together with the corresponding varying temperature field at the middle of the panel at opposite sides

The tip-displacement evolution shows extreme deep and sharp notches. Convergence checks on the time step size have been executed. Nevertheless, these notches are numerically not convenient.

The displacement field and the corresponding temperature field for one of the moments with highest deformation of the panel are presented in Figure 8 and Figure 9.

3.2.3 Selection of responses and design variables

For many instruments the peak-to-peak variation of the deformation is of interest, because it provides the range of deformation. In this example, the maximum and minimum tip displacement are taken for that reason as performance results and the influence of stochastic design variables on the extreme displacement values are assessed. Therefore, in the following, the maximum and minimum values of the displacement over the

transients are presented as responses of interest. Note that in this case the maximum value represents the smallest negative displacement and minimum the highest negative displacement. The minimum and maximum values are obtained by scanning over the transient data and searching for the highest and lowest value of the Y-displacement of the mid-point at the +Z edge of the panel.

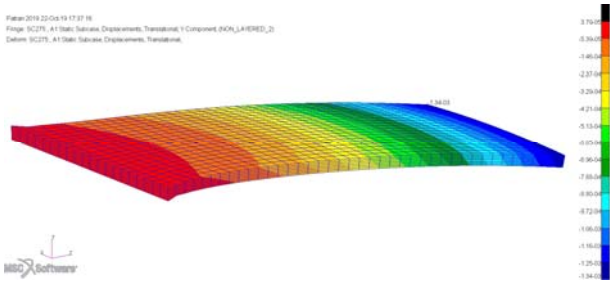

Figure 8 Thermally induced displacements

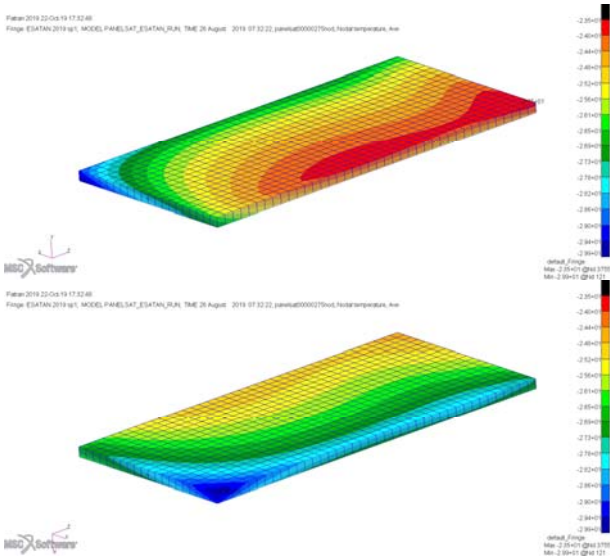

Figure 9 Temperature field at nadir side (top picture) and zenith side (bottom picture) of panel value within the dispersion range at the moment with the highest deformation.

In this example the following model properties are taken as stochastic design variables:

- t_{nadir} and t_{zenith}: The face sheet thicknesses of the nadir and zenith side of the panel. Both model properties are considered as independent stochastic design variables. These parameters affect the stiffness of the panel as well as the face sheet conductance and heat capacity.
- k_{core}: The conductivity of the core material, which affects both the through thickness and the in-plane conductance.
- ε_{nadir} and ε_{zenith}: The infra-red emissivity of the two sides of the panel. Also, these parameters are considered independent stochastic design variables. The parameters affect the infra-red radiative heat exchange with the planet and deep space. It must be noted that when these parameters change, the corresponding infra-red reflectivity has to be changed accordingly.
- α_{nadir} and α_{zenith}: The solar absorptivity of the two sides of the panel. Also, these parameters are considered independent stochastic design variables. The parameters affect the absorption of direct solar and albedo radiation. Also here the corresponding solar reflectivity has to be changed when these parameters change.
- CTE_{nadir} and CTE_{zenith}: The coefficients of thermal expansion of the nadir and zenith face sheet material. These are considered to be two independent design variables. One could consider this situation to be relevant when the material of the two face sheets is coming from two different manufacturing batches or when the material appears to be not homogeneous.

The fact that the CTE_{nadir} and CTE_{zenith} for the two face sheets are considered as independent variables implies that both variables can be in their opposite extremes (one at the smallest and one at its highest value in the variation range). This might lead to high ranges in deformation responses.

The above list of design variables means that in total, nine stochastic design variables are used. All the other material and geometrical properties are kept at their nominal level.

In Table 4 nominal or mean values of the stochastic design variables, that are used for the PANELSAT example, are presented.

To find out what the impact is on the minimum and maximum tip-displacement due to random variation of the above listed stochastic design variables, both Monte Carlo Simulation is used as well the $2k+1$ PEM method.

As is explained in section 2.2 care must be taken with selection of the size of the dispersion of the stochastic design variables when the $2k+1$ PEM method is used. For this reason, different values of the dispersion of the stochastic design variables have been investigated.

Table 4 Nominal values of stochastic design variables

Design Variable	Nominal/Mean value
t_{nadir}	0.001 m
t_{zenith}	0.001 m
k_{core}	8.5 W/mK
ε_{nadir}	0.5
ε_{zenith}	0.8
α_{nadir}	0.5
α_{zenith}	0.2
CTE_{nadir}	2.32E-5 m/m/K
CTE_{zenith}	2.32E-5 m/m/K

All the stochastic design variables are assumed to have a uniform probability distribution around the mean value that is considered to be equal to the nominal value. In this example, the dispersion is expressed as a percentage of the mean value. So

when a dispersion of 10% is indicated, it means that the lower-bound is at 90% of the mean values and upper-bound is at 110% of the mean value.

The percentages of dispersion that are used are 10%, 5%, 2.5% and 1.25% and are applied to all design variables simultaneously.

3.2.4 Stochastic analyses

For each of these dispersion values, the $2k+1$ PEM method is applied. The Monte Carlo simulation was run in parallel to act as a reference value for the estimates produced by the $2k+1$ PEM method of the computed stochastic properties of the two responses: The minimum and maximum edge displacement. For the Monte Carlo simulations for each magnitude of dispersion 1800 analyses were executed. Within each MCS run, all nine stochastic variables were sampled. With both the Monte Carlo and the $2k+1$ PEM method computed, the mean and standard deviation of the minimum and maximum tip-displacement are estimated and presented for the different dispersion levels in Figure 10 and Figure 11.

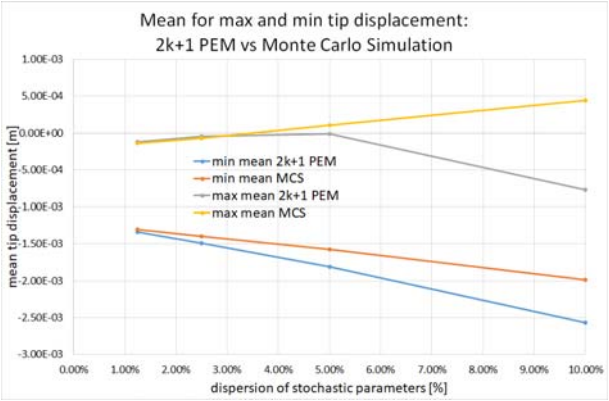

Figure 10 Correlation of the mean for maximum and minimum tip displacement (with among others 2 independent CTE design variables)

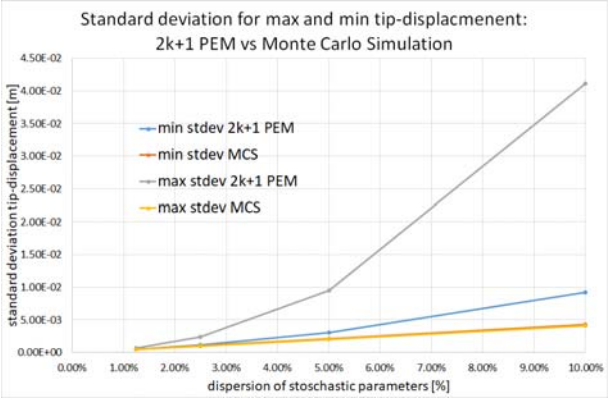

Figure 11 Correlation of the standard deviation for maximum and minimum (with among others 2 independent CTE design variables)

From Figure 11 it can be observed that the curves for the standard deviations produced with the Monte Carlo runs appear to be linear functions of the dispersion. When the problem is not too non-linear, this is what would be expected. In this example all design variables appear only in a linear form in the response equations. It is therefore to be expected that standard deviation is proportional to the dispersion of the stochastic design variables. This gives confidence that an adequate amount of analyses were done with the Monte Carlo approach to produce this property and that therefore the results of these analyses can be used as reference to judge the quality of the estimates produced with the $2k+1$ PEM method.

What can be observed clearly from Figure 11 is that the curves of the standard deviation for the $2k+1$ PEM method do not have this linear behaviour and are even estimating for a dispersion of 10% a standard deviation of more than 4 cm for the maximum value of the tip-displacement. This is not a realistic value and also for a dispersion of 5% the produced standard deviation 9.5 mm is a non-physical value. For the dispersion levels of 5% and 10% it may well be that for this example for some of the design variables the dispersion level is too high.

From Figure 10 can be observed as well that the mean values are also not well correlating. For the 10% dispersion of the design variables, the mean and standard deviation for the tip displacements is numerically compared in Table 5.

Table 5 Mean and standard deviation for minimum and maximum tip displacement for dispersion of 10% with CTE parameters comparing the $2k+1$ PEM method and Monte Carlo (MCS)

	min $2k+1$	min MCS	max $2k+1$	max MCS
μ	-2.565E-03	-1.987E-03	-7.721E-04	4.454E-04
σ	9.191E-03	4.297E-03	4.112E-02	4.112E-03

An additional interesting observation is that the mean and standard deviation of the MCS results do not match with the one of a fitted normal distribution (compare the mean and standard deviation in the column “min MCS of Table 5 with the values in Figure 12).

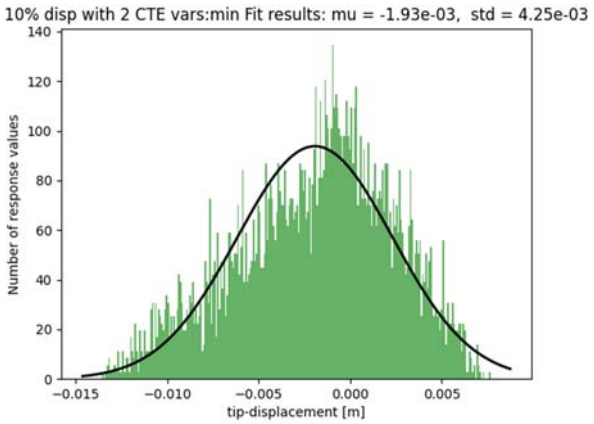

Figure 12 Fitted normal distributions to minimum tip-displacements produced with the MCS method (with among others 2 independent CTE design variables)

Also a level of skewness in the distribution of the

response values can be observed in Figure 12.

Rosenblueth [1] indicates in his paper that his method requires that the distribution of the design variables shall have no skewness. This requirement is adhered to. However, it is not clear to what extent the skewness in the response distributions are responsible for the unrealistic values for the standard deviation. It is also not yet clear what is causing the skewness that is observed

The question now is which design variables are causing these unrealistic values?

To answer this question, use can be made of the coefficient of variation values V_n the response due to variation of each individual parameter that have been calculated for the computation the standard deviation of the responses (see Equation (4)). In Table 6 these values are presented for the response of minimum and maximum tip-displacement for the case in which design variables have a 10% dispersion.

Table 6 Coefficient of variation $|V_n|$ of the minimum and maximum tip displacement for dispersion of 10% using the $2k+1$ PEM method.

Var #	Design Variable	$\|V_n\|$ for minimum	$\|V_n\|$ for maximum
1	t_{nadir}	2.40E-03	4.26E-02
2	t_{zenith}	1.29E-03	3.51E-02
3	k_{core}	5.57E-02	5.23E-02
4	ε_{nadir}	1.90E-03	2.12E-03
5	ε_{zenith}	4.14E-02	1.20E-01
6	α_{nadir}	1.68E-02	9.87E-02
7	α_{zenith}	3.32E-03	1.45E-01
8	CTE_{nadir}	1.63E+00	7.15E+00
9	CTE_{zenith}	1.67E+00	7.12E+00

The results of Table 6 show that the CTE design variables have by far the highest values for the coefficients of variation and are therefore expected to be the driving parameters behind the excessively high standard deviations for the response of the tip-displacement. There is therefore a high likelihood that the dispersion of these design variables are causing the $2k+1$ PEM method estimate to be off. To have this confirmed a case with again a dispersion of 10% is run, but this time leaving out the design variables CTE_{nadir} and CTE_{zenith}. Since for the $2k+1$ PEM method all the Y_{nm} and Y_{np} values are already available, it is quite straightforward to compute the estimates for the mean and standard deviation without the influence of the CTE design variables. It is however needed to rerun all the cases for the MCS analysis for the set of parameters without the CTE design variables.

Table 7 Mean and standard deviation for minimum and maximum tip displacement for dispersion of 10% <u>without CTE</u> parameters comparing the $2k+1$ PEM method and Monte Carlo (MCS)

	min $2k+1$	min MCS	max $2k+1$	max MCS
μ	-1.252E-03	-1.256E-03	-1.931E-04	-1.947E-04
σ	8.970E-05	9.154E-05	4.400E-05	4.426E-05

In Table 7 the estimates for the mean and standard deviation are presented without the influence of the CTE parameters, but still with a dispersion level of 10%. The results show that without the design variables CTE_{nadir} and CTE_{zenith}, but maintaining the high dispersion of 10% for the remaining design variables the $2k+1$ PEM method estimate is reproducing quite well the Monte Carlo results.

Trying to fit again the data from the Monte Carlo simulation with a normal distribution it can be seen that the fitted normal distribution matches also well the stochastic properties of the Monte Carlo results (compare the mean and standard deviation in the column “min MCS of Table 7 with the values in Figure 13). Also no obvious sign of skewness in the response of the minimum tip-displacement is visible.

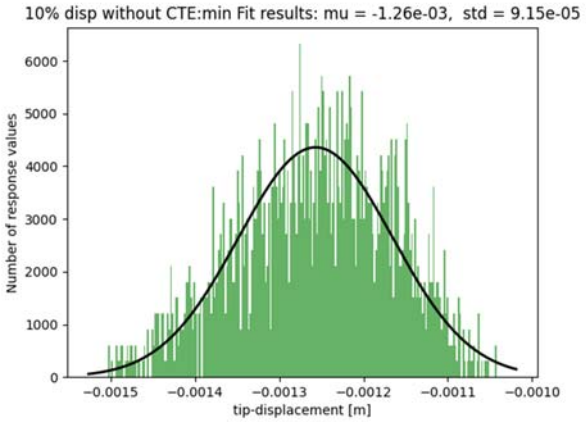

Figure 13 Fitted normal distributions to minimum tip-displacements produced with the MCS method <u>without CTE</u> design variables

So there is definitely something going on that is caused by the two CTE design variables.

So far two independent design variables were considered for the CTE for the zenith and nadir face sheet. With a dispersion of 10%, it is possible to have sample combinations of both design variables that differ up to 20%. This is extremely high. It would imply a not so well controlled manufacturing process of the face sheets or the two face sheets are coming from two different material suppliers, which is quite rare.

The choice of having two independent design variables for the CTE design variables also implies that bending of the panel can occur even when the panel has a uniform temperature. With a dispersion level of 10% for each of the CTE design variables,

this is most likely too much for the $2k+1$ PEM method for the current example.

From Figure 10 and Figure 11 it can be learned that when the dispersion levels are reduced in magnitude the deviation between the MCS and $2k+1$ PEM method is also significantly reduced to a level that could be considered acceptable for a dispersion of 2.5%.

It must be noted that for this example case the structure is subjected to more than 60 degree of temperature variation relative to the reference temperature. The high temperature excursion is likely to amplify the effect of CTE difference in top and bottom face sheet.

The above consideration have led to the hypothesis that with a single CTE design variable for the both the zenith and nadir face sheet above observed problems with the results would be reduced. To verify this hypothesis, a dedicated analysis with a 10% dispersion level for all design variables is again run. This time CTE_{nadir} and CTE_{zenith} are one to one correlated and have in each analysis the same value. This implies that there are now 8 instead of 9 independent design variables. For the $2k+1$ PEM method this means that only 17 analysis runs have to be performed. The MCS is also repeated with 1800 runs, sampling values for the 8 design variables.

In Table 8 the mean and standard deviation are compared with for both the MCS and $2k+1$ PEM method. This case there is almost perfect correspondence between both methods.

Table 8 Mean and standard deviation comparing the $2k+1$ PEM method and Monte Carlo (MCS) for minimum and maximum tip displacement for dispersion of 10% with a single CTE design variable associated to top and bottom face sheet

	min $2k+1$	min MCS	max $2k+1$	max MCS
μ	-1.252E-03	-1.256E-03	-1.925E-04	-1.930E-04
σ	1.115E-04	1.224E-04	4.489E-05	6.745E-05

Trying to fit again the data from the Monte Carlo simulation with a normal distribution it can be seen that the fitted normal distribution matches well the stochastic properties of the Monte Carlo results (compare the mean and standard deviation in the column “min MCS of Table 8 with the values in Figure 14). A slight trace skewness may be observed. This may also be caused by the “just” 1800 result values.

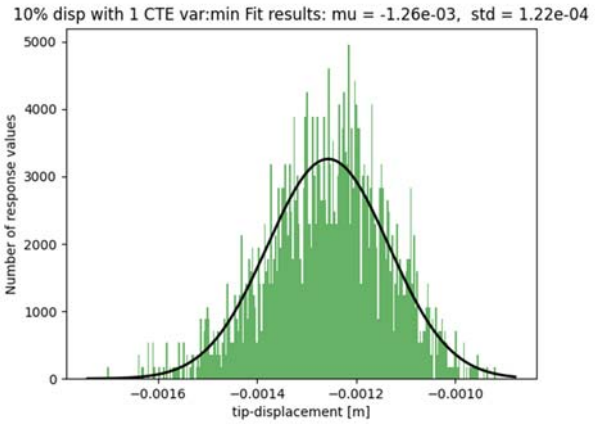

Figure 14 Fitted normal distributions to minimum tip-displacements produced with the MCS method with a single CTE design variable

3.2.5 Concluding remarks on the example

This example shows the strength of the $2k+1$ PEM method compared to the Monte Carlo Simulation method. Instead of the 1800 simulation runs for the Monte Carlo simulation only 17 cases for the 8 design variables are sufficient to accurately reproduce the results. Even when the 17 cases have to be repeated, the number of analysis cases is still manageable with a little effort. The example showed that limitations of the method can be reached and how this can be detected.

In this example it was quite obvious that the dispersion level of two of the design parameters was affecting the quality of the estimates for the mean and the standard deviation of the responses. It might not always be that obvious. In this case the Monte Carlo Simulation results were available for reference and showed a proportional relation between the standard deviation of the responses and the standard deviation of the input variables.

When no reference MCS results are available, the proportionality verification, as a way to verify the validity of the dispersion value, has then to be performed by generating additional results with the $2k+1$ PEM method. These results are obtained through an extra set of runs in which the dispersion levels of the design variables are scaled by a factor 2 or 0.5. The corresponding estimates of the standard deviation of the responses should then show the same scaling factor. If this proportionality is not demonstrated, then the values of the coefficients of variation for the different design variables (for instance a list similar to Table 6) may help to identify which of the design variables may be causing the problem.

The experience with the $2k+1$ PEM method for thermoelastic problems in the space industry is still quite limited. Further application of the method will extend the experience and will provide more guidelines on the use of the method.

4 CONCLUSION AND RECOMMENDATIONS

At the moment, there is no ECSS handbook providing guidelines for thermoelastic verification and consequently also none on the treatment of uncertainties in thermoelastic predictions.

The $2k+1$ PEM method offers the potential to obtain the uncertainty in the responses with a strongly reduced computational effort. As an example running uncertainty analysis on a full spacecraft with 50 design variables would require "only" 101 analysis runs. This would be a more feasible number compared to thousands of runs that would be needed with the Monte Carlo Simulation method.

A nice side product of the method are the coefficients of variation of the response for each design variable. These coefficients can be considered a measure of the sensitivity of the response variables with respect to the design variables. Furthermore, it requires only two additional runs to get the coefficients of variation when the sensitivity information for an extra design variable is needed. In comparison, the Monte Carlo Simulation method would require, probably, several hundreds of extra analyses.

The method has limitations that were faced on the second example in this paper. One of the limitations of the $2k+1$ PEM method that was already indicated by Rosenblueth is that the dispersion of the design variables shall not be too large. A way to check this is to verify whether the standard deviation of the response variable is proportional to the standard deviation of the design variables.

The examples presented in this paper are relatively small. More experience with more complex models is to be gained with this method. The authors hope that this paper inspires the community to try the method as well and share their findings. In this way the application of the method can develop to a mature method that can complement the approach of factors of safety.

5 ACRONYMS AND ABREVIATIONS

CPT	Centre Point Temperature interpolation method
FPA	Focal plane assembly
MCS	Monte Carlo Simulation
PAT	Prescribed Average Temperature interpolation method
PEM	Point Estimate Method
SC	Spacecraft
TE	Thermoelastic
TN	Thermal node

6 REFERENCES

1. E. Rosenblueth. Two-point estimates in probability. Applied Mathematical Modelling, 5:329–335, October 1981.
2. A.S. Nowak and K.R. Collins. Reliability of Structures. ISBN 0-07-116354-9. McGraw-Hill, 2000.
3. Alfredo H-S. Ang, Wilson H. Tang, Probabilistic Concepts in Engineering, Emphasis on Applications to Civil and Environmental Engineering, 2nd edition, John Wiley & Sons, Inc. ISBN 978-0-471-72064-5
4. A. Olsson, G. Sandberg, O. Dahlblom, ON Latin hypercube sampling for structural reliability analysis, Structural safety, Vol. 25, pages 47-68, 2003.
5. John. T. Christian, Gregory B. Baecher, The point-estimate method with large numbers of variables, Int. J. Numer. Anal. Meth. in Geomech., Vol. 26. Pages 1515-1529, 2002 (DOI: 10.1002/nag.256)
6. ECSS-E-ST-32-10C Rev.1, 6 March 2009, Structural factors of safety for spaceflight hardware
7. M. Koot, S. Appel, and S Simonian. Thermal Conductor Generation for Thermal and Thermo-Elastic Analysis using Finite Element Model and SINAS. In European Conference on Spacecraft Structures, Materials & Mechanical Testing. ESA/ESTEC, CNES, DLR, 2018.
8. ECSS-E-HB-31-03A, November 15th 2016, Thermal analysis handbook
9. M. Koot, S. Appel, and S. Simonian. Temperature Mapping for Structural Thermoelastic Analysis; Method Benchmarking. In European Conference on Spacecraft Structures, Materials & Mechanical Testing. ESA/ESREC, CNES, DLR, May-June 2018.
10. Menno Koot et al. Accurate Thermal Mapping and Finite Element Model Based Conductor Generation; Extended Method Benchmarking Guidelines. In European Space Thermal Engineering Workshop. ESA/ESTEC, Oct 2018.
11. Department of Defense. Metallic materials and elements for aerospace vehicle structures. 2003.
12. Jochen Doenecke. Survey and Evaluation of Multilayer Insulation Heat Transfer Measurements. 1993.
13. Jarque Carlos M. and Bera Anil K. Efficient tests for normality, homoscedasticity, and serial independence of regression residuals. 1980.